KSME Journal, Vol. 4, No. 2, pp. 167~171, 1989.

INVESTIGATION OF THE FLOW FIELD DEVELOPED BEHIND A PLANAR SHOCK WAVE PROPAGATING INTO A REACTIVE GAS SOLID SUSPENSION

M. Olim*, G. Ben-Dor*, M. Mond* and O. Igra*

(Received December 16, 1989)

The equations governing the flow-field which is developed when a moderately strong shock wave propagates in an oxygen-carbon suspension were developed and solved numerically. The energy transfer which takes place between the shocked gas and the solid carbon particles causes ignition of the particls. The resulting flow-field properties are shown at different times.

Key Words: Shock Wave Propagation, Gas-Solid Suspension, Reacting Flow(Combustion), Ignition

1. INTRODUCTION

A schematic description of the considered flow is given in Fig. 1. At $t<0$ the normal shock wave propagates in pure gas. At $t=0(x=0)$ the normal shock wave enters the dusty suspension(oxygen seeded with carbon particles).

As long as the shock wave moves in pure gas it maintains a constant velocity, and the post-shock flow properties can be calculated through the Rankine-Hugoniot relations if the pre-shock flow conditions and the Mach number of the shock wave are known. Ahead of the shock wave the suspension is in a state of thermodynamic equilibrium, i.e. the temperature and the velocity of the oxygen are equal to those of the carbon particles. The passage of the shock wave through the suspension causes almost instantaneous changes in the velocity, pressure, density, and temperature of the gaseous phase. On the other hand the solid phase is practically unaffected by the shock front since the diameter of the solid particles is much larger than the shock thickness. In the present study the particle diameter is 100×10^{-6}m, whereas the shock thickness is of the order of several mean free paths which is about 0.1×10^{-6}m. As a result immediately behind the shock front the two phases are no longer in equilibrium. The temperature of the gas is higher than that of the particles and it moves at the appropriate shock induced velocity, whereas the carbon particles remain at rest and at their initial temperature. Intense processes of energy and momentum transfer take place between the two phases change the temperature of the carbon reaches its ignition point, a combustion process starts. The combustion continues until the carbon particles are completely burnt out. Therefore, the entire flow-field can be divided into three regions:

(1) The pre-shock region where the suspension is in a state of complete equilibrium.
(2) The relaxation zone which starts immediately behind the shock front. In this zone momentum and energy transfer between the two phases take place. Also, if the temperature of the carbon is high enough, combustion takes place.
(3) A new state of equilibrium is reached when the processes occurring in the relaxation zone are over.

In the derivation of the conservation equations describing the flow-field it was assumed that:
(1) The flow-field is unsteady and one-dimensional.
(2) For purposes excluding momentum and energy transfer between the gas and the solid particles, the gaseous phase is considered as inviscid and heat non-conductive.
(3) The combustion products are instantly mixed in the oxygen gas to result in uniform temperature and velocity of the gaseous phase at any given cross-section of the flow-field.
(4) The carbon particles are solid spheres uniformly distributed in the gaseous phase at any given cross-section. They retain their spherical shape at any time.
(5) Based on the Biot number of the particles, it is assumed that the particle temperature is uniform.
(6) The volume occupied by the carbon oparticles is negligibly small in comparison with the volume of the suspension.
(7) Due to the low number density of the particles in the suspension, interactions between them are ignored.
(8) The only force acting on the particles is the drage force.
(9) The combustion process is described by two simultaneous reactions:

$$2C+O_2 \overset{r_1}{\Longrightarrow} 2Co+h1 \tag{1}$$

$$C+CO_2 \overset{r_2}{\Longrightarrow} 2Co+h2 \tag{2}$$

where r_1 and r_2 are the rates of the first and the second reactions, and $h1$ and $h2$ are the amounts of heat released in the first and the second reactions. An additional reaction occurs between the various species of the gaseous phase:

$$2CO+O_2 \overset{r_3}{\Longrightarrow} 2CO_2+h3 \tag{3}$$

where r_3 is the reaction rate, and $h3$ is the amount of heat released in this reaction.

*Pearlstone Center for Aeronautical Engineering Studies, Department of Mechanical Engineering, Ben-Gurion University of the Negev, Beer Sheva, Israel

(10) $h1$, $h2$, and $h3$ are independent of the suspension pressure or temperature.
(11) The heat released by the above mentioned reactions is absorbed solely by the the gaseous phase.
(12) Due to the relatively large convection velocities all diffusion processes are neglected.

Based on these assumptions the conservation equations are:
Continuity of the gaseous phase species,

$$\frac{\partial}{\partial t}(\rho_i)+\frac{\partial}{\partial x}(u\rho_i)=\frac{d}{dt}(\rho_i) \tag{4}$$

In the case of carbon combustion the gaseous phase is composed of O_2, CO, and CO_2 and therefore the equation of continuity of the gaseous phase contains three equations: $i=1$ for O_2, $i=2$ for CO, and $i=3$ for CO_2. ρ_i is the i-th species and $\frac{d}{dt}(\rho_i)$ is the rate of production of the i-th species due to the reactions listed in assumption 9.

Momentum balance of the gaseous phase,

$$\frac{\partial}{\partial t}(\rho u)+\frac{\partial}{\partial x}(\rho u^2+P)=-F \tag{5}$$

Energy balance of the gaseous phase,

$$\frac{\partial}{\partial t}[\rho(C_V T_g+0.5u^2)]+\frac{\partial}{\partial x}\{u[\rho(C_V T_g+0.5u^2)]+P\}=-(Q+VF) \tag{6}$$

Continuity of the solid phase,

$$\frac{\partial}{\partial t}(\rho_p)+\frac{\partial}{\partial x}(\rho_p V)=\frac{d}{dt}(\rho_p) \tag{7}$$

Momentum balance of the solid phase,

$$\frac{\partial}{\partial t}(\rho_p V)+\frac{\partial}{\partial x}(\rho_p V^2)=F \tag{8}$$

Energy balance of the solid phase,

$$\frac{\partial}{\partial t}[\rho_p(CT_p+0.5v^2)]+\frac{\partial}{\partial x}[\rho_p v(CT_p+0.5V^5)]=Q+VF \tag{9}$$

Conservation of the number density of the carbon particles,

$$\frac{\partial}{\partial t}(n)+\frac{\partial}{\partial x}(nV)=0 \tag{10}$$

In these equations ρ, u, T_g, and P are the gaseous phase density, velocity, temperature, and pressure, respectively, where $\rho=\sum\rho_i \cdot \rho_p$, T_p, v, and n are the carbon spatial density, temperature, velocity, and number density, respectively. $\frac{d}{dt}(\rho_p)$ is the rate of change of the carbon spatial density due to the combustion. F, Q, C, and C_V are the drag force per unit volume acting on the solid phase, the heat transferred per unit volume from the gaseous phase to the solid phase, the specific heat capacity of the carbon, and the specific heat capacity of the gaseous phase at constant volume, respectively. The above set of equations contains 9 equations with 10 unknowns, which are the flow-field properties: $\rho_1, \rho_2, \rho_3, u, T_g, P, \rho_p, v, T_p$ and n. The additional equation required to make the above set of equations solvable is the euqation of state of the gaseous phase, i.e.

$$P=\rho R T_g \tag{11}$$

where R is the gas constant. At any given cross-section of the flow-field a single carbon particle mass m_p is calculated by: $m_p=\rho_p n^{-1}$, and its diameter D is calculated by $D=[6m_{pa}(\pi\sigma)^{-1}]^{1/3}$ where σ is the material density of the carbon particles. In principle, the set of Eqs.(4) ~ (11) is now solvable. However, the terms $\frac{d}{dt}(\rho_i)$, $\frac{d}{dt}(\rho_p)$, C, C_V, F, and Q have to be expressed in terms of the unknown flow-field properties. The rates of production/consumption of the various suspension species depend upon the the reactions describing the chemical reactions. Sundaresan and Amundson (1980) suggested that:

$h1=221MJ$ $\quad r_1=0.0363\rho_1\exp(-17967/T_p)$
$h2=-172.8MJ$ $\quad r_2=9.13\times10^6\rho_3\exp(-29790/T_p)$
$h3=283MJ$ $\quad r_3=5.12\times10^6\rho_1^{0.5}\rho_2\exp(-15098/T_g)$

Reactions r_1 and r_2 are per unit area and therefore should be multiplied by the solid phase surface area. The surface area A of a carbon particle can be calculated from its diameter. Therefore,

$$\frac{d}{dt}(\rho_1)=(-0.5r_3-nAr_1)M_1 \tag{12}$$

$$\frac{d}{dt}(\rho_2)=[2(r_1+r_2)nA-r_3]M_2 \tag{13}$$

$$\frac{d}{dt}(\rho_3)=(-nAr_2+r_3)M_3 \tag{14}$$

$$\frac{d}{dt}(\rho_p)=-nA(2r_1+r_2)M_p \tag{15}$$

where M_1, M_2, M_3, and M_p are the molecular weights of O_2, CO, CO_2 and carbon, respectively. The suspension pressure is calculated using the Dalton law of partial pressures, i.e. $P=\sum P_i$. The partial pressure P_i of each of the species composing the gaseous phase if found using its equation of state, i.e., $P_i=\rho_i R_i T_g$ where R_1, R_2, and R_3 are the specific gas constants of O_2, CO, and CO_2 respectively.

The drag force per unit volume acting upon the solid phase can be expressed as

$$F=0.125\pi n\rho C_d|u-v|(u-v)D^2 \tag{16}$$

The particle drag coefficient C_d is a function of Reynolds number Re. The correlations adopted for the present solution were suggested by Clift et. al. (1978). For $Re<800$

$$C_d=\frac{24}{Re}(1+0.15Re^{0.687}) \tag{17}$$

and for $Re\geq800$

$$C_d=\frac{24}{Re}(1+0.15Re^{0.687})+\frac{1}{1+42500Re^{-1.16}} \tag{18}$$

Reynolds number is defined as $Re=\rho D|u-v|\mu^{-1}$. The viscosity of the gaseous phase μ is calculated using the values of the viscosity of the various species composing this phase: $\mu=(\sum\mu_i\rho_i)\rho^{-1}$ C_V can be calculated using the values of the

specific heat capacity of each of the species of the gaseous phase, i.e. $C_v=(\sum C_{vi}\rho_i)\rho^{-1}$ where C_{v1}, C_{v2}, and C_{v3} are the specific heat capacity at constnat volume of O_2, CO, and CO_2 respectively. C_{vi} are functions of the gas temperature only. The correlations used in the present solutions were suggested by van Wylen and Sonntag(1978)

$$C_{v1}=1169.8+6.282\times10^{-4}T_g^{1.5}-5580487T_g^{-1.5}+74027313T_g^{-2}-R_1 \quad (19)$$

$$C_{v2}=2468.6-0.7955T_g^{0.75}-71677.97T_g^{-0.5}+199559.16T_g^{-1.75}-R_2 \quad (20)$$

$$C_{v3}=-84.883+69.371T_g^{0.5}-0.93238T_g+5.4983\times10^{-5}T_g^2-R_3 \quad (21)$$

The heat absorbed/released by the gaseous phase(Q) is the sum of the heat produced/consumed in the chemical reactions listed in assumption 9 and the heat transferred to the carbon particles(Q_p)

$$Q=An(h_1r_1+h_2r_2)+h_3r_3-Q_p \quad (22)$$

$$Q_p=An[(T_g-T_p)h+\bar{\sigma}(T_g^4-T_p^4)] \quad (23)$$

where h and $\bar{\sigma}$ are the heat convection coefficient and the Stephan-Boltzmann constant, respectively. The coefficient h can be expressed in terms of the Nusselt number of the gaseous phase and its thermal conductivity: $h=NukD^{-1}$ where Nu is the Nusselt number and k is the thermal conductivity that can be calculated from $k=(\sum k_i\rho_i)\rho^{-1}$ where k_1, k_2, and k_3 and $k_3$are values of the thermal conductivity of O_2, CO, and CO_2 respectively. The thermal conductivity of the gaseous phase components is temperature dependent, and the following functions were fitted to discrete data given by Samsonov(1973):

$$k_1=-8.91\times10^{-4}+1\times10^{-4}T_g-2.51\times10^{-8}T_g^2 \quad (24)$$

$$k_2=4.61\times10^{-3}+6.32\times10^{-5}T_g-6.54\times10^{-9}T_g^2 \quad (25)$$

$$k_3=-6.51\times10^{-3}+7.72\times10^{-5}T_g \quad (26)$$

The Nusselt number is calculated from a correlation suggested by Drake(1961):

$Nu=2+0.459Pr^{1/3}Re^{0.55}$. Pr is the Prandtl number $Pr=\mu C_pk^{-1}$ where C_p is the the specific heat capacity at constant volume of the gaseous phase calculated using $C_p=(\sum C_{pi}\rho_i)\rho^{-1}$. The specific heat capacity of carbon is a function of temperature, and a function was fitted to discrete data given by Stull et al.(1971):

$$C=1429.16-0.3555T_p-73.2\times10^{-6}T_p^{-2} \quad (27)$$

2. SOLUTION METHOD

The flow-field is described by 9 partial differential conservation equations in 10 unknowns. The 10th equation is an algebraic equation of state that relates the gas pressure to its density and temperature. The conservation Eq.(4) to (10) can be written in the following vector form:

$$\boldsymbol{\phi}_t+\boldsymbol{\Psi}(\boldsymbol{\phi})_x=\boldsymbol{\zeta} \quad (28)$$

where $\boldsymbol{\phi}_t, \boldsymbol{\Psi}(\boldsymbol{\phi})$,and $\boldsymbol{\zeta}$ are vectors, and the subscripts t and x denote partial differentiation with respect to time and to the space coordinate, respectively. The vector Eq.(28) was solved using the operator splitting technique, according to which the solution is done in two steps. The first step is to solve the conservative part of Eq.(28):

$$\boldsymbol{\phi}_t+\boldsymbol{\Psi}(\boldsymbol{\phi})_x=0 \quad (29)$$

which was solved using the Flux Corrected Transport(FCT) method(Book, Boris & Hain, 1975). The FCT method was developed especially to treat discontinuous functions, and is of second order of accuracy in time and space.

The second step of the solution of Eq.(28) includes the mechanical and the chemical interactions between the flow-field components:

$$\boldsymbol{\phi}_t=\boldsymbol{\zeta} \quad (30)$$

Equation(30) was solved using the predictor-corrector method: the values of the flow-field properties obtained from the solution of Eq.(29) (known values) were used to solve Eq.(30)to caculate the values of the flow-field properties at the next time level(predicted values), then intermediate time level values were calculated by avergaging the known and the predicted values. These average values were used to calculate the vecotr $\boldsymbol{\zeta}$ and the final (corrected) values of the flow-field properties at the next time level were calculated from Eq.(30). The predictor-corrector method is of second order of accuracy, therefore the combined algorithm is of second order of accuracy in both time and space.

To check the reliability of the convective part of the numerical scheme, the Riemann problem was solved numerically. The results were compared with the analytical solution and showned excellent agreement. To check the relibility of the combined algorithm, a problem where a shock wave travels into an inert particle-gas suspension was solved and the results were compared with experimental results presented by Sommerfeld, 1985. Good agreement was obtained. No experimental results of shock waves traveling into areactive particle-gas suspension were available for comparison.

3. RESULTS

The inital conditions of the studied case were: for $-\infty<X<0$ the one dimensional flow-field contains pure oxygen. For $0<X<\infty$ the one dimensional flow-field contains oxygen and uniformly distributed spherical carbon particles. A shock wave of Mach number 5.0 travels from the negative side of the x axis towards the right as shown in Fig. 1, The oxygen ahead of the shock wave is stationary($u=0$), at atmospheric pressure(0.1 MPa) and its temperature is 300°K. The carbon particles are in thermal and kinematic equilibrium with the oxygen($v=u=0$, $T_p=T_g$). The carbon particles are of a singel diameter of 100×10^{-6}m, and the ratio of the spatial density of the carbon to the initial oxygen density is 0.05.

The chemical reaction between the carbon and the oxygen is negligible if the carbon temperautre is below 1000°K (Sundaresan and Amundson, 1980). Therefore, after the

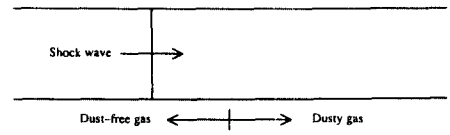

Fig. 1 Schematic description of flow

shock wave has entered the carbon laden gas, there is a finite period of time in which energy and momentum are transferred from the gas to the particles but no combustion occurs. The gas loses momentum to the solid phase and consequently its density increases. Fig. 2 shows the carbon temperature 3×10^{-3}, 6×10^{-3}, 9×10^{-3}, and 12×10^{-3} seconds after the shock wave has entered the oxygen-carbon suspension (times are shown in milliseconds in all figures). No carbon is found in regions where $T_p=0$.

As can be seen from Fig. 2, the carbon temperature after 3×10^{-3} seconds is below 1000°K. Therefore, no chemical reaction has taken place. At later times, the carbon temperature is above 1000°K and chemicla reaction between the oxygen and the carbon occur in the suspension.

Figure 3 shows the oxygen density at the same times. The oxygen density immediately behind the shock wave increases monotonically at all times. This increase in the oxygen density is due to the loss of momentum to the solid phase. A depletion of the oxygen density can be seen in these regions of the flow-field in which chemical reactions occur ($t=6\times10^{-3}$, 9×10^{-3}, and 12×10^{-3} seconds).

Fugure 4 shows the pressure of the gaseous phase 3×10^{-3}, 6×10^{-3}, 9×10^{-3}, and 12×10^{-3} seconds after the shock wave has entered the suspension.

A monotonic increase is observed in the pressure immediately behind the shock wave. $Att=3\times10^{-3}$ this increase is due solely to the momentum loss to the solid phase. At later times, this pressure increase is partially due to the momentum loss and partially due to the heat generated by the combustion process. Comparison of Figs. 3 and 4 showns that at any time the lowest oxygen density values are found at the points of highest pressure. The reason for this is that the lowest values of oxygen density are located in the regions of the most intense combustion, which are the regions of the most intense heat production. Heat released to the gaseous phase by the chemical reactions causes a temperature increase, which increases the pressure.

Figure 5 shows the velocity of the gaseous phase 3×10^{-3}, 6×10^{-3}, 9×10^{-3}, and 12×10^{-3} seconds after the shock wave has entered the suspension.

At $t=3\times10^{-3}$ a decrease in the gas velocity immediately behind the shock wave is observed. This is due to the loss of momentum to the solid phase. At later times, it is observed that the gas velocity immediately behind the shock wave increases and that it decreases in some other regions of the flow-field. Comparison of Figs. 4 and 5 shows that the gas velocity is high in the regions of the flow-field which are located between the pressure peaks and the shock wave and that the gas velocity is low in the regions that follow the pressure peaks, thus showing an expected relationship between the pressure gradients and the acceleration.

Figure 6 shows the velocity of the solid phase 3×10^{-3}, 6×10^{-3} 9×10^{-3}, and 12×10^{-3} seconds after the shock wave has entered the suspension.

Analysis of the figures showing the gas and the carbon velocities and the carbon temperature (Figs. 5, 6, and 2)

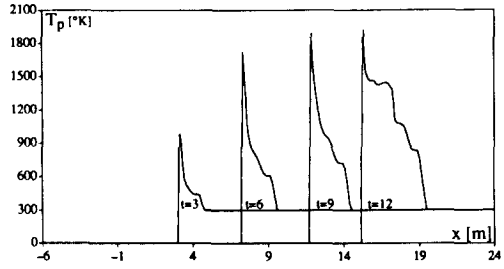

Fig.2 Carbon temperature with time after the schock wave

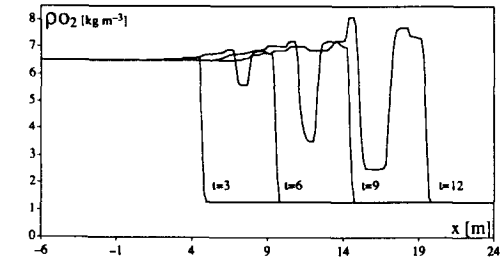

Fig.3 Oxygen density with time after the schock wave

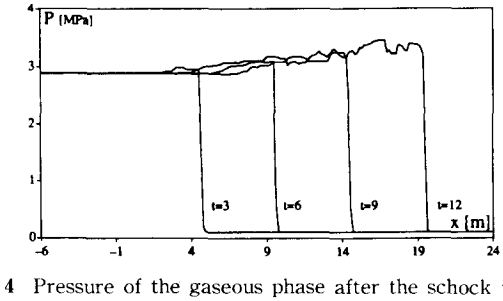

Fig.4 Pressure of the gaseous phase after the schock wave

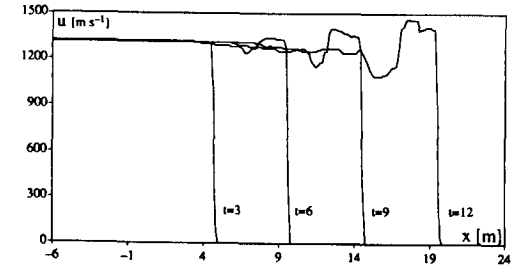

Fig.5 Velocity of the gaseous phase after the schock wave

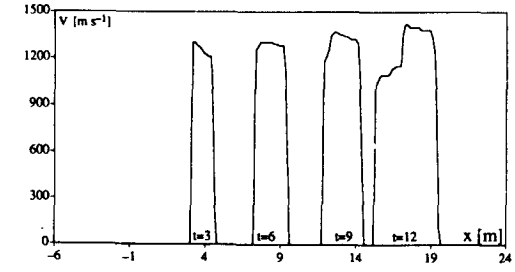

Fig.6 Velocity of the solid phase after the schock wave

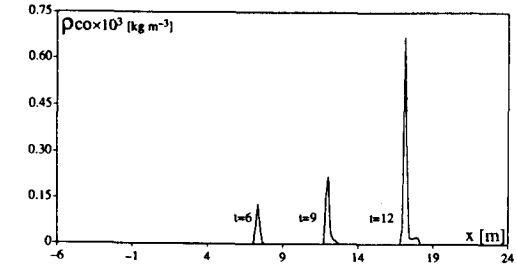

Fig.7 Densities of CO

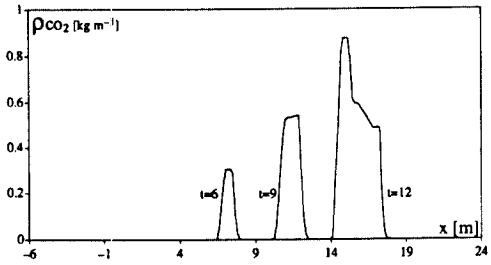

Fig.8 Densities of CO_2

shows that the velocity of the solid particles reaches the gas velocity before the ignition temperature is reached. Therefore, the burining particles are convected at the same velocity as the gas surrounding them. The energy released by the combustion is absorbed by the surrounding gas, thus increasing its temperature. Increase of the gas temperature causes increase of the carbon temperature, thus accelerating the combustion process. The densties of the two gaseous combustion products (CO and CO_2) are shown in Figs. 7 and 8, respectively.

Comparison of Figs. 7 and 8 shows that the density of CO is much lower than the density of CO_2. It also shows that CO is being consumed by the reaction which produces. CO_2. The combined density of all the gaseous components in the regions of intense combustion is lower than the original oxygen density, which implies that the pressure peaks are due to the high gas temperature rather than to the additional gaseous components released into the suspension by the chemical processes.

4. CONCLUSIONS

The momentum exchange that takes place between the gaseous and the solid phases causes a decrease in the gas velocity immediately behind the shock wave. This deceleration of the gas causes an increase in the gas density. The energy exchange between the two phases causes a decrease in the gas temperauture immediately behind the shock wave. These changes in the gas temperauture and density have contradiction effects on the gas pressure. In the case in vestigated here the gas pressure has increased, as can be seen at time $=3\times10^{-3}$ seconds(before the combustion starts). However, it is possible that different particle diameters and/or loading factors will have a different effect upon the gas pressure. Since the flow behind the shock wave is subsonic with respect ot the shock wave, the pressure peak that develops after the combustion starts causes an increase in the pressure immediately behind the shock wave and accelerates the gas behind the shock wave, thus strengthening the shock wave. The carbon combustion is a self-accelerating process since part of the heat released by it is returned to the carbon particles by convection and radiation from the gas, thus accelerating the chemical reactions. The pressure peaks in regions of intense combustion are mainly due to the temperature increase of the gaseous mixture rather than to the additional mass of the combustion products.

REFERENCES

Book, D.L., Boris, J.P. and Hain, K., 1975, "Flux Corrected Transport 2, Generalization of the Method," J. Comp. Phys., Vol. 18 pp. 248~283.

Clift, R., Grace, J.R. and Weber, M.E., 1978, "Bubbles, Drops, and Particles," Academic Press, New-York.

Samsonov, G.V., 1973, "The Oxyde Handbook," Plenum, New-York.

Sommerfeld, M., 1985, "The Unsteadiness of Shock Wave Propagating Through Gas-Particle Mixtures," Exps. Fluids, Vol. 3, pp. 197~206.

Stull, D.R. et al., 1971, "JANAF Thermodynamical Tables," US Department of Commerce, National Bureau of Standards.

Sundaresan, S. and Amundson, N.R., 1980, "Diffusion and Reaction in Stagnant Boundary Layer About a Carbon Particle. 5, Pseudo-Stady State. Structure and Parameter Sensitivity," Ind. Eng. Chem. Fund., Vol. 19, pp. 344~351.